Experimental study of the weak field Zeeman spectra of ^{85}Rb and ^{87}Rb

A Wyngaard[1], G De Jager[2], C Steenkamp[3] and K Govender[4]

[1,4] Department of Electrical, Electronic and Computer Engineering, Cape Peninsula University of Technology, Bellville, Cape Town, 7535, South Africa

[2] Department of Electrical Engineering, University of Cape Town, Cape Town, 7701, South Africa

[3] Department of Physics, University of Stellenbosch, Stellenbosch, 7599, South Africa

E-mail: [1] 210176296@mycput.ac.za

Abstract. We report on the measurement and analysis of the magnetic sub-levels of rubidium 85 and 87 that are observed in the presence of a weak magnetic field. Included is the standard hyperfine interaction. The experiment was performed using a saturated absorption spectroscopy setup with a set of Helmholtz coils placed around the rubidium vapour cell in order to generate a magnetic field. An external cavity diode laser was frequency modulated and the output split into three beams, two weak probe beams and a strong pump beam which counter-propagates and overlaps one of the probe beams. These beams were sent through a rubidium vapour cell where a magnetic field was applied. The time axis of each oscilloscope capture was converted to frequency using a calibration factor determined through previously measured values for hyperfine peak separations. The converted spectra were fitted with Lorentzian curves to estimate energy level separations, and the experimental and theoretical magnetic sub-level separation was plotted as a function of the magnetic field.

1. Introduction

It has been shown that there are multiple approaches to analysing the Zeeman shift in the magnetic hyperfine structure of rubidium (Rb) [1, 2]. A possible application of the Zeeman effect has been demonstrated in the investigation of low-field magnetometry [3]. These studies typically depend on comparing experimental results with predictions that are based on the average effects of interactions between electrons, and between electrons and the nucleus; thus, results may vary for multi-electron atoms.

Our study looked at the energy level separation for two magnetic energy levels of ^{85}Rb and ^{87}Rb in the presence of a weak magnetic field. The study was limited to using linearly polarised light, where the transitions between magnetic levels are those for which $\Delta m_F = 0$.

This study forms part of a larger experiment involving the cooling and trapping of Rb atoms using a magneto-optical trap. Since such an experiment requires knowledge of the energy structure of Rb and how the structure is affected by magnetic fields, investigating the Zeeman effect served as an ideal method for gaining such knowledge.

2. Theory

In the presence of an external magnetic field, the degeneracy associated with levels specified by the m quantum number is removed. These magnetic levels have energies that are a function of the magnetic field. At the hyperfine stage each level denoted by the quantum number F is split into $2F+1$ magnetic levels denoted by m_F. This magnetic hyperfine structure is shown in Figures 1 and 2. Also shown in these figures are the transitions between $F = 3$ and $F' = 4$, and $F = 2$ and $F' = 3$; for which $\Delta m_F = 0$, which is the special case we consider in this paper.

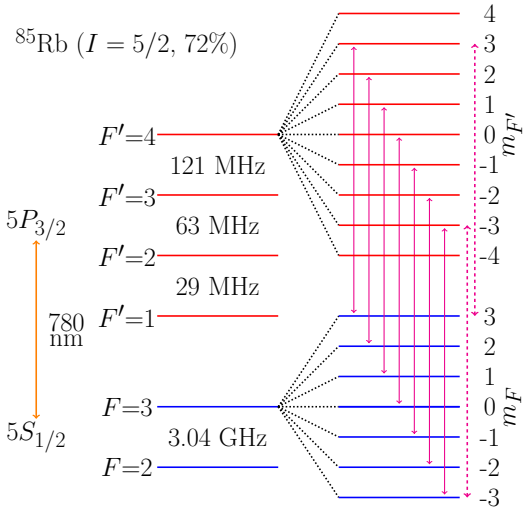

Figure 1. ^{85}Rb $F = 3$ to $F' = 4$ magnetic hyperfine structure. Ground states are denoted by F, excited states are denoted by F', and magnetic states are prefixed with m. Only the transitions for linearly polarised light are shown (solid arrows). The dashed arrows are explained in Section 4.2.

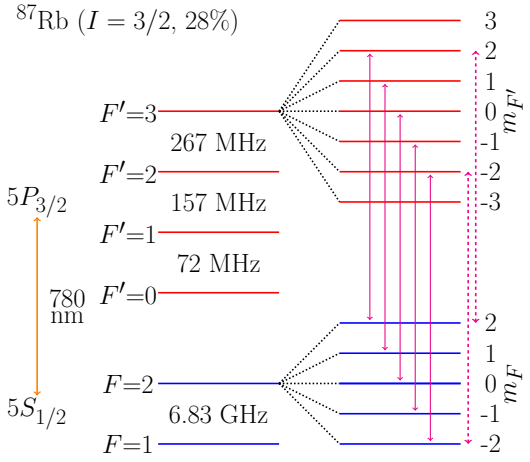

Figure 2. ^{87}Rb $F = 2$ to $F' = 3$ magnetic hyperfine structure. Ground states are denoted by F, excited states are denoted by F', and magnetic states are prefixed with m. Only the transitions for linearly polarised light are shown (solid arrows). The dashed arrows are explained in Section 4.2.

In the weak field regime, where the internal magnetic field is dominant, the orbital and spin angular momenta remain coupled and the Hamiltonian is given by

$$H = \underbrace{\left[H_0' + \zeta(r)\vec{L}\cdot\vec{S}\right]}_{H_0} + \underbrace{A\vec{I}\cdot\vec{J} + \frac{\mu_B}{\hbar}\left(g_J\vec{J} + g_I\vec{I}\right)\cdot\vec{B}}_{H'} \tag{1}$$

where H_0 is the basic atomic Hamiltonian including the spin-orbit coupling (fine structure), H' represents the interaction between the nucleus and electron (hyperfine structure), and the magnetic dipole moments of the atom interacting with an external magnetic field $\vec{B}$, A is a constant, μ_B is the Bohr magneton, and g_J and g_I are the g-factors [4, 5].

Taking a closer look at H' in Equation (1),

$$H' = A\vec{I}\cdot\vec{J} + g_J\frac{\mu_B}{\hbar}\vec{J}\cdot\vec{B} + g_I\frac{\mu_B}{\hbar}\vec{I}\cdot\vec{B}\ , \tag{2}$$

we see the hyperfine structure energy $A\vec{I}\cdot\vec{J}$ which is due to the interaction of the nuclear spin with the magnetic field created by the orbiting electron, and two more terms which are a

function of the external magnetic field. These two terms are the energy contributions from the magnetic levels due to the interaction of the net orbital and spin dipole moment of the electron with an external magnetic field, and the interaction of the nuclear spin dipole moment with an external magnetic field. The quadrupole interaction term has been neglected in our analysis of the magnetic hyperfine energy levels.

3. Experimental Setup

A saturated absorption setup was used to measure the hyperfine energy levels. The setup is shown in Figure 3. It consists of a Rb vapour cell which is illuminated by a strong pump beam that is linearly polarised by the half-wave plate (HWP) and polarising beam splitter (PBS) combination. The pump beam is then reflected by a mirror, attenuated by a neutral density (ND) filter, and the polarisation is rotated 90 degrees by a quarter-wave plate (QWP) before passing back through the Rb cell. This beam now acts as a probe beam which is monitored by a photodetector. We linearly scan the frequency of the laser to cover the range needed and we use a Michelson interferometer to determine the separation between hyperfine levels. This separation is then used to calibrate measurements of the magnetic hyperfine levels.

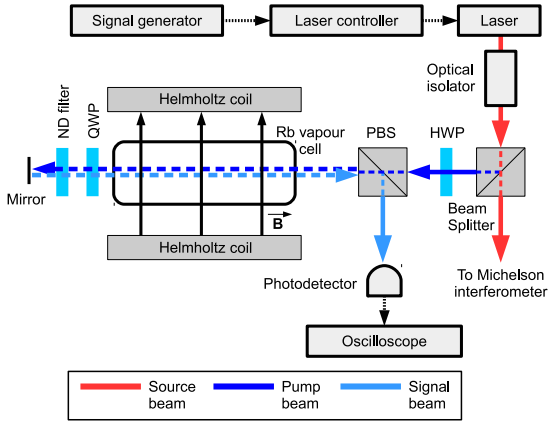

Figure 3. Saturated absorption spectroscopy setup with a set of Helmholtz coils that are used to generate a uniform magnetic field across the Rb vapour cell.

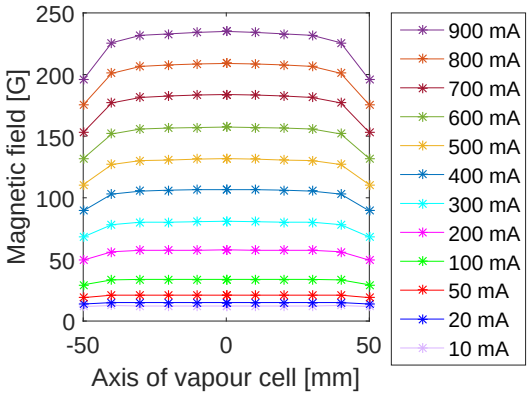

Figure 4. Various magnetic field strengths measured at several positions between the Helmholtz coils. The Rb cell is in the -40 to 40 mm region.

To examine the Zeeman effect we added a set of Helmholtz coils such that the magnetic field is perpendicular to the laser beams. The magnetic field across the Rb cell was measured for various current settings, as shown in Figure 4. In the region of the Rb cell (-40 to 40 mm), the field is approximately constant.

4. Results

4.1. Computational Analysis

Using the uncoupled basis $|J\, m_J\, I\, m_I\rangle$ to diagonalise the Hamiltonian matrix H' described in Section 2, we obtained the energy levels of the hyperfine magnetic sub-levels at various values of $\vec{B}$. Figures 5 and 6 show plots of the $5S_{1/2}$ and $5P_{3/2}$ energy levels of ^{87}Rb for several values of $\vec{B}$, a similar analysis has been done for ^{85}Rb but is not shown. The predictions agree with those given by others [3, 4, 5].

This computational analysis of the energy shift between magnetic levels was then compared to our experimental analysis of Zeeman spectra acquired from a saturated absorption setup.

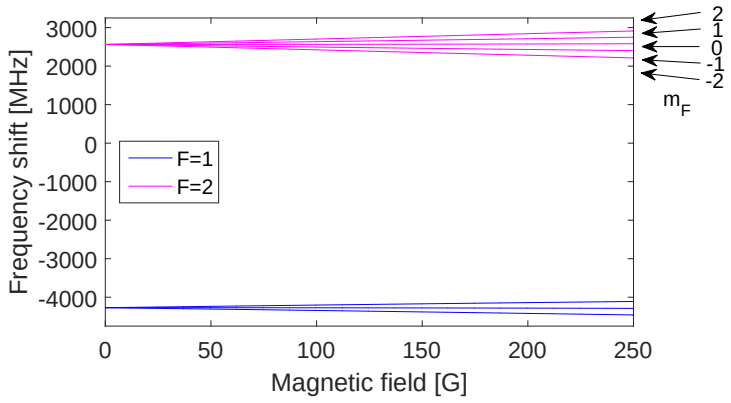

Figure 5. ^{87}Rb $5S_{1/2}$ magnetic hyperfine structure for several values of $\vec{B}$. The arrows indicate the magnetic energy levels, denoted by m_F, for the $F = 2$ ground state.

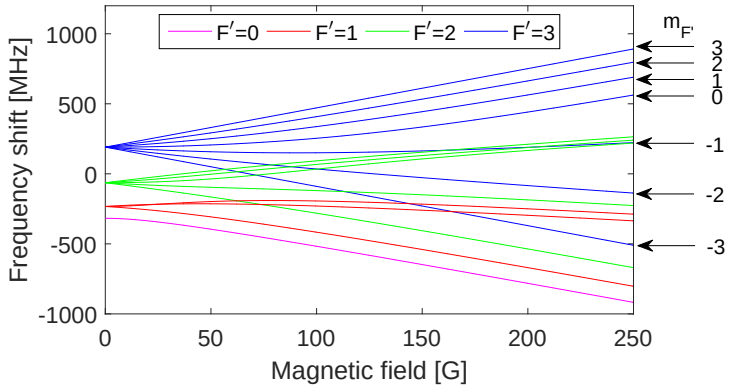

Figure 6. ^{87}Rb $5P_{3/2}$ magnetic hyperfine structure for several values of $\vec{B}$. The arrows indicate the magnetic energy levels, denoted by $m_{F'}$, for the $F' = 3$ excited state.

4.2. Experimental Analysis

In Figure 7 we show the hyperfine spectrum for ^{85}Rb as the laser frequency is varied. This spectrum corresponds to transitions from $F = 3$ to $F' = 2, 3, 4$ in Figure 1. For the Zeeman analysis we focused on the rightmost hyperfine peak corresponding to the $F = 3$ to $F' = 4$ transition. The spectrum in Figure 8 corresponds to ^{87}Rb transitions from $F = 3$ to $F' = 2, 3, 4$, shown in Figure 2. Here we focused on the rightmost hyperfine peak for Zeeman analysis, this peak corresponds to the $F = 3$ to $F' = 4$ transition.

Figures 9 and 10 show sequences of the splitting of the hyperfine peaks as the magnetic field is varied. We measured the separation between these peaks and compared them with those obtained from the computational analysis shown in Figures 5 and 6. This is shown in Figures 11 and 12. For ^{85}Rb the measured values correspond to the difference in transition energy from level $m_F = 3$ to $m_{F'} = 3$ and $m_F = -3$ to $m_{F'} = -3$, indicated by dashed arrows in Figure

1. In the case of ^{87}Rb the measured values correspond to a difference in transition energy from level $m_F = 2$ to $m_{F'} = 2$ and $m_F = -2$ to $m_{F'} = -2$, indicated by dashed arrows in Figure 2.

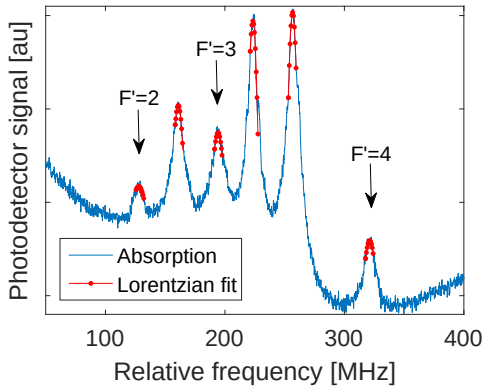

Figure 7. Saturated absorption spectrum of ^{85}Rb showing hyperfine transitions from $5S_{1/2}$ $F = 3$ to $5P_{3/2}$ $F' = 2$, 3, 4.

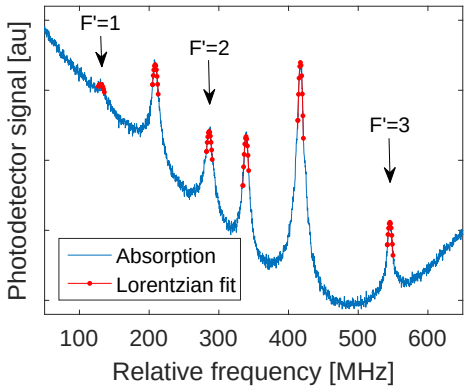

Figure 8. Saturated absorption spectrum of ^{87}Rb showing hyperfine transitions from $5S_{1/2}$ $F = 2$ to $5P_{3/2}$ $F' = 1$, 2, 3.

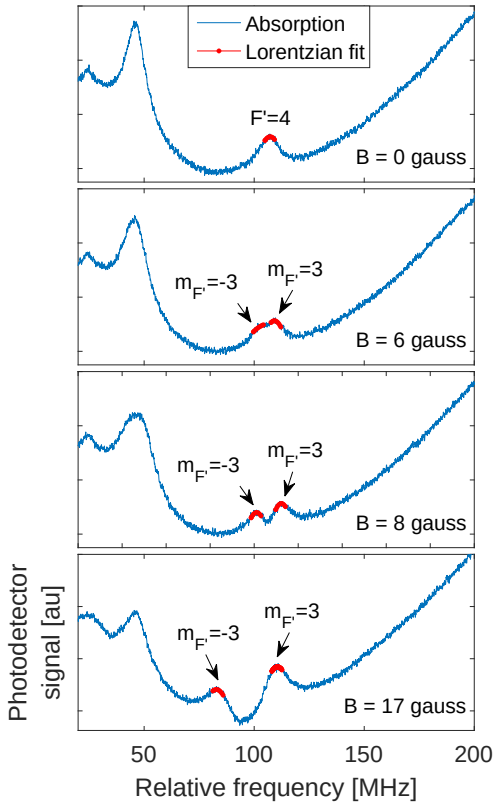

Figure 9. Saturated absorption spectrum of ^{85}Rb showing the transition from $5S_{1/2}$ $F = 3$ to $5P_{3/2}$ $F' = 4$. As the magnetic field is increased, $5P_{3/2}$ $F' = 4$ splits into magnetic sub-levels, $m_{F'} = -3, 3$.

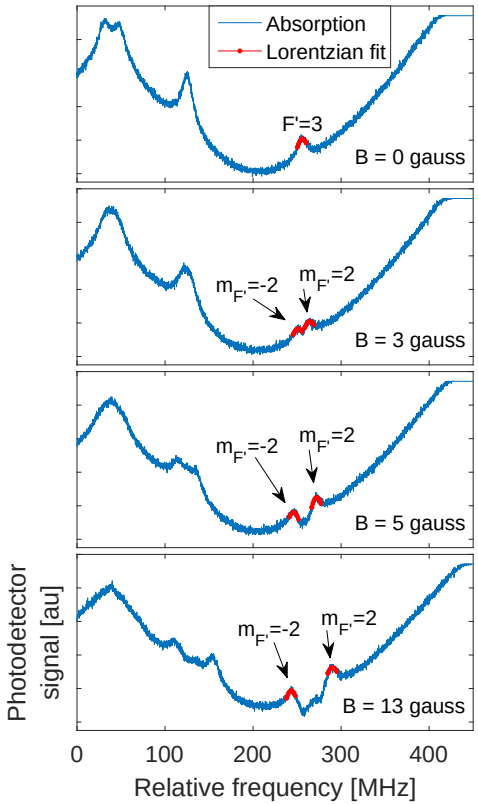

Figure 10. Saturated absorption spectrum of ^{87}Rb showing the transition from $5S_{1/2}$ $F = 2$ to $5P_{3/2}$ $F' = 3$. As the magnetic field is increased, $5P_{3/2}$ $F' = 3$ splits into magnetic sub-levels, $m_{F'} = -2, 2$.

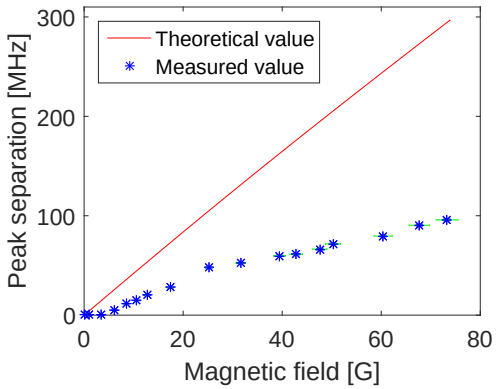

Figure 11. Computational versus experimental shift in frequency for the ^{85}Rb $5S_{1/2}$ $F = 3$, $m_F = -3, 3$ to $5P_{3/2}$ $F' = 4$, $m_{F'} = -3, 3$ magnetic hyperfine transitions. The uncertainty of each measurement is given as green bars.

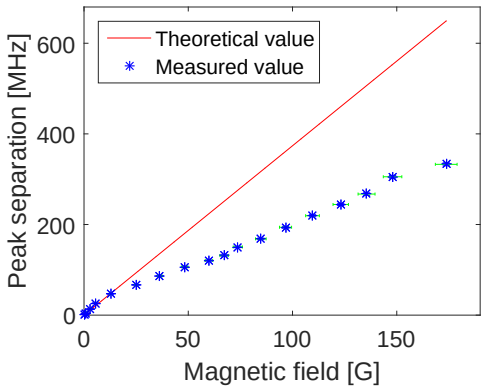

Figure 12. Computational versus experimental shift in frequency for the ^{87}Rb $5S_{1/2}$ $F = 2$, $m_F = -2, 2$ to $5P_{3/2}$ $F' = 3$, $m_{F'} = -2, 2$ magnetic hyperfine transitions. The uncertainty of each measurement is given as green bars.

5. Summary

We have demonstrated an experimental setup for the investigation of the Zeeman effect on the magnetic hyperfine structure of ^{85}Rb and ^{87}Rb. An analysis of the theoretical and experimental data shows large variations for both ^{85}Rb and ^{87}Rb. The difference between theoretical and experimental values is greater for ^{85}Rb. This may be due to the fact that we have neglected the quadrupole interaction in our theoretical analysis of the Zeeman effect; this interaction may need to be considered as it is larger for ^{85}Rb than ^{87}Rb, due to the higher nuclear spin value.

Additionally, the theory is an approximation which considers the average effects of interactions between electrons as well as between electrons and the nucleus, this may lead to inconsistencies between the prediction and experiment for multi-electron atoms such as rubidium.

References

[1] Bowie J, Boyce J and Chiao R 1995 *J. Opt. Soc. Am. B* **12** 1839–1842
[2] Kim J, Kim H, Moon H and Lee H 1997 *J. Opt. Soc. Am. B* **14** 2946–2947
[3] Ram N, Pattabiraman M and Vijayan C 2007 *J. Phys. Conf. Ser.* **80** 1–10
[4] Steck D 2013 Rubidium 85 d line data available online at URL `http://steck.us/alkalidata (revision 2.1.6, 20 September 2013)`
[5] Steck D 2015 Rubidium 87 d line data available online at URL `http://steck.us/alkalidata (revision 2.1.5, 13 January 2015)`